



## Conjugated Polymer /Multi Wall Carbon Nanotubes Composite Characterisation for Application in Volatile Organic Compounds Sensors

<sup>1</sup>Yahaya, M.I., <sup>2</sup>Shams B. al-Atraqchi

<sup>1</sup>Chemistry Department, Sokoto State University, Sokoto, Nigeria.

<sup>2</sup> Department of Laser and Electro-optics Engineering, University of Technology, Baghdad, Iraq.

### Article info

Received: Nov 28, 2021

Revised: July 23, 2022

Accepted: July 25, 2022

#### Keywords:

Volatile Organic Compounds,  
Carbon Nanotubes,  
Composite,  
Sensor,  
Conductivity.

### Abstract

Composites of conjugated polymers (CP) are becoming increasingly used in nanoelectronics devices, due to their electronic and optical properties. Recent efforts have demonstrated that the incorporation of materials like carbon nanotubes (CNTs) that have excellent physical and chemical properties, within the matrix of CP could improve the sensing proficiency. The monitoring of pollutants for human health, as they can cause several diseases, is an important aspect of research, and the detection of toxic species is an issue of growing interest. A lot of research work on the application of CP/CNTs composite in gas sensing have been conducted but more research is needed to explore their potentials as sensing elements. The aim of our work is to use a simple chemical and low cost method to coat CNTs with polyimidazole polymer (Plm) and test their ability to sense pollutants. Polyimidazole multi-walled carbon nanotubes (Plm/MWCNTs) nanocomposite film were synthesised by chemical oxidation of imidazole monomer and addition of MWCNTs to the conductive polymer (CP) solution in 1:1 ratio. Chemical characterisation using FTIR where there is an increased in intensity of peaks in the control sample from 2823 and 2937  $\text{cm}^{-1}$  to 2833 and 2947  $\text{cm}^{-1}$  in Plm/MWCNTs composite respectively and Raman spectroscopy in which Plm/MWCNTs shows the so-called D-band (attributed to disordered  $\text{sp}^2$  and non- $\text{sp}^2$  carbon defects in graphitic sheets) and G-band (attributed to the C–C vibration with the  $\text{sp}^2$  hybridised orbital in graphene structures) peaks at 1355  $\text{cm}^{-1}$  and 1593  $\text{cm}^{-1}$ , but chemical analysis confirmed the mixing of the polymer and the MWCNTs. Electrical measurements using current voltammetry (CV) that shows a reversible wave that is the typical behaviour of conductive surfaces in the presence of the redox couple and Impedance measurements in which the largest semicircle was obtained with Plm/CNTs film that corresponds to a film resistance on the real axis of 350  $\text{M}\Omega$  which is an indication of a higher electron transfer rate in the redox probe and good electrical behaviour. The overall results have shown that the composite has a significant electrical conductivity and can be applied in sensing volatile organic compounds in the environment.

### 1. Introduction

Scientific and technological communities globally have great interest in materials that can form well-defined materials on the nanometre scale. The unique properties which materials exhibit when one or more of their physical dimensions are so reduced presents great potential for their exploitation in

different applications [1-2].

Composites of conjugated polymers are becoming increasingly used in organic electronics devices, due to the electronic and optical properties of the polymers, which are like those of semiconductors. However, the mechanical properties and processability of polymers makes them more attractive than

crystalline inorganic semiconductors for future applications: their low weight, flexibility and inexpensive preparation procedures are drawing the attention of many researchers [3-4]. Because of the ensuing reason, it is not surprising that the properties of composites of conjugated polymers which have been formed by addition of either a macromolecule or nanometer-sized inorganic within the material should be of interest to researchers.

In the presence of these inserted materials, new nanoscale polymer structures can form that lead to new and interesting physical properties. Due to their flexibility, lightweight and corrosion resistance, composites composed of electromagnetic fillers and polymer matrix are gaining popularity as microwave-absorbing materials. Among these conductive fillers, CNTs have been widely studied due to their excellent physical and chemical properties [5-6].

The outstanding electrical, mechanical, and thermal properties of carbon nanotubes (CNTs) have made them among the most promising materials in a wide range of applications such as nanosensors and atomic transportation. In addition, the excellent mechanical properties of CNTs, such as ultra-high Young's modulus around and tensile strengths are promising ultra-high-strength reinforcements in high-performance polymer matrix composites [7-8].

Recent efforts have demonstrated that the incorporation of secondary materials like metals or metal oxides, nano-particles and carbon nanotubes (CNTs) within the matrix of conductive polymer or its derivatives could improve the sensing proficiency as a result of combined effects of the components. Athawale and co-workers observed good sensitivity and selectivity of the palladium/PANI nanocomposite sensor toward methanol vapour at low vapour concentration (4 ppm). However, the nanocomposite sensor possessed weak sensitivity at < 4 ppm methanol concentration. As reported by Kulkarni, the sensing performances of PANI to ethanol vapour were significantly improved upon

inclusion of small concentrations of silver (Ag) nanoparticles. However, the PANI/Ag nanocomposite sensor exhibited poor response and inferior reproducibility [9-10].

Carbon nanotubes are promising materials because of their unique physical properties for example, high surface area, the length compared to the diameter which is between (0.5-20) nm, high aspect ratio with a high conductivity and stable in high temperatures (up to 1000 K). Therefore, CNTs are used in many applications, for example industrial, medical. In the sensing application carbon nanotubes appeared to have a weak response to sense chemical vapour, for example acetone, propanol. It has been informed that the sensitivity of carbon nanotubes increased after decorating with nanoparticles such Ag or with adding different types of polymer such as polypyrrole [11-12].

Gas pollutants are a set of different gases which can be encountered in the ambient and that can be dangerous to human health. The monitoring of these pollutants for human health, as they can cause several diseases, is an important aspect of research, and in fact, the detection of toxic species is an issue of growing interest. The vapour of volatile organic compounds (VOCs) released from different industrial processes are among the pollutants of environmental concern due to their toxic potentials when in higher concentration in the ambient [13].

Gas sensors are devices that can change the concentration of an analyte gas into an electronic signal; it is composed of an active sensing material with a signal transducer. Electrochemical sensors have more advantage over others because; their electrodes can sense the materials which are present within the host without doing any damage to the host system. Chemical sensors have become an important part of our technology driven society and can be seen in chemical processes, medicine monitoring of environmental pollutants, dangerous waste, warfare agents, disease diagnostics, food quality, industrial safety and

indoor monitoring among others. Notwithstanding, gas sensor technologies are still developing and have yet to reach their full potentiality in capabilities and operation. Thus, there are strong demands for highly selective, sensitive, cost effective, stable, and robust VOCs nanosensors [14-15].

Last three decades, chemical sensor systems have been used for monitoring of environmental pollutants, hazardous waste materials, warfare agents, disease diagnostics, food quality and industrial safety. The chemical sensors systems are being developed to have advantages like fast, portable, reliable, harmless, and most importantly non-destructive means of detection for contamination, especially in food products. The vapour of volatile organic compounds (VOCs) like acetone, methanol, ethanol, chloroform, toluene, among others released from chemical industry, pharmaceutical industry, food industry and polymer industry, is responsible for air pollution. The conducting polymers-based sensors, which have added advantage over the classical inorganic semiconductor, can be readily introduced to detect the varying VOCs at lower concentrations with better selectivity at room temperature [16].

A lot of research work on the application of CP/CNTs composite in gas sensing have been conducted but more research is needed to explore their potentials as sensing elements. The aim of our work is to use a simple chemical and low cost method to coat CNTs with polyimidazole polymer (Plm) and test their ability to sense VOCs at room temperature. In this research imidazole was used to coat MWCNTs to study the sensing properties of CNTs at room temperature. The films were prepared by drop casting. Imidazole is an organic compound with a 5-member ring.

## 2. Experimental

### 2.1 Materials

Imidazole was purchased from Sigma-

Aldrich Company Ltd.;  $\text{FeSO}_4 \cdot 7\text{H}_2\text{O}$  and CNTs were provided by Thomas Swan Company, and  $\text{MgCl}_2 \cdot 7\text{H}_2\text{O}$  was obtained from BDH Chemicals Ltd. Lambda DNA was purchased from New England Biolab. All the chemicals were of AnalaR grade or equivalent. Silicon wafer, was purchased from Compart Technology Ltd. Microband electrodes were supplied by Windsor Scientific Ltd. Copper grids for TEM were purchased from EM Resolutions Ltd. Deionised water was obtained from a Nano pure Diamond Life Science ultrapure water system equipped with a Reverse Osmosis System and were used for all the experiments.

### 2.2 Substrates cleaning

Using a diamond scribe, silicon wafers were cut into  $\sim 1 \times 1 \text{ cm}^2$  pieces and immersed in acetone for 50 minutes. They were then rinsed with plentiful deionised water and dried in a gentle stream of Nitrogen gas before further drying in an oven for 5 - 10 minutes. FEMTO low pressure plasma system was used for final cleaning, using oxygen plasma oxidation (90W, 15 sccm, 15 min) at 40% power.

### 2.3 Chemical synthesis of Polyimidazole

Polyimidazole was chemically synthesised as explained in [17]. 5  $\mu\text{L}$  of freshly prepared imidazole (solution (1 mM) was added to 5  $\mu\text{L}$  of  $\text{MgCl}_2$  (0.5 mM), then 5  $\mu\text{L}$  of  $\text{FeCl}_3$  (1mM) was added dropwise into the solution. The solution was thoroughly mixed and allowed to react for at least 2 h at room temperature.

### 2.4 Preparation of CNT/Plm Composite

MWCNTs was mixed with 10 ml of methanol and sonicated (25 - 3) h to disperse the nanotubes. 20  $\mu\text{L}$  of the prepared polyimidazole was added to 20  $\mu\text{m}$  of MWCNTs (1:1) and the solution was left for 2 hours [18].

### 2.5 Electrical measurements

Cyclic voltammograms test is used to

study the electro-chemical property of the hybrid nanotubes. The electrical analysis was done by EStar with scan rate 0.05 v/s, voltage window (-0.5 – 0.7) Volt and current range between 1 to 100  $\mu\text{A}$ . all the samples were deposited on microband electrons.

## 2.6 Fourier transform infrared measurements

5  $\mu\text{L}$  of Plm/MWCNTs was deposited on treated Si chip by drop casting approach and dried at room temperature. The IRAffinity-1S spectrometer was used to study the structure properties of the nano films carried out on a DTG detector with wavelength range between 400 to 4000  $\text{cm}^{-1}$  and resolution of 16  $\text{cm}^{-1}$ .

## 2.7 Raman spectrophotometric measurements

Raman experiments were conducted using Witec (Alpha 300R–Confocal Raman Imaging) and CCD KL1500 LCD was used to collect the results with a wavelength 488 nm laser diode, 60 mWatt, wavenumber range between 0 to 3100  $\text{cm}^{-1}$ . The technique is used to study the level of interaction/mixing of the CP and CNTs.

## 3. Results and Discussion

### 3.1 FTIR results analysis

The characteristic functional groups in MWCNTs and Plm/CNTs composite are

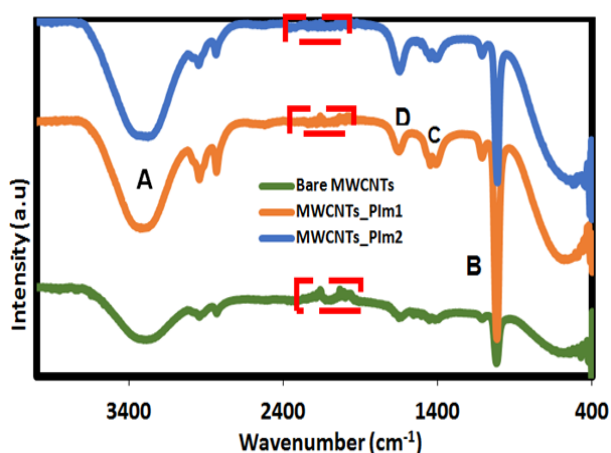


Fig. 1: FTIR Transmission spectra of Plm/MWCNTs (Blue and Orange) vs. bare MWCNTs (controls). 128 scans co-added and averaged, 4  $\text{cm}^{-1}$  resolutions.

revealed in their FTIR spectra in Figure 1. Broad absorption peaks were observed in the wavenumber 3282  $\text{cm}^{-1}$  (A) for both MWCNTs (control) and Plm/MWCNTs composite which is assigned to bonding vibration of water molecules due to moisture absorption by samples [19]. There is an increase in intensity of peaks in the control from 2823 and 2937  $\text{cm}^{-1}$  to 2833 and 2947  $\text{cm}^{-1}$  in Plm/MWCNTs composite respectively. The C-H stretch at 2131  $\text{cm}^{-1}$  (red square) in MWCNTs (control) disappeared in Plm/MWCNTs composite. The amine N-H bending for imidazole was observed at 1645  $\text{cm}^{-1}$  (D) in the Plm/MWCNTs composite indicating the mixing of the two substances. Infrared spectrum peak at 1432  $\text{cm}^{-1}$  (C) in control shifted to 1402  $\text{cm}^{-1}$  in the Plm/MWCNTs composite indicating C-N stretching.

The peak at 1030  $\text{cm}^{-1}$  (B) which is due to the C=O stretching frequency, indicated the presence of a carboxylic group created during the oxidation of MWCNTs [20]. The intensity signifies the presence of a number of carboxylic groups which had been attached successfully to the surface of MWCNTs after mixing. The FTIR result indicates strong interaction between MWCNTs and Plm/MWCNTs composite and hence the formation of the hybrid composite.

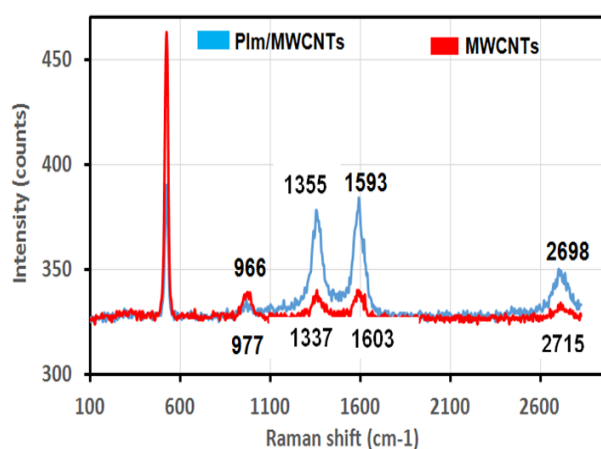


Fig. 2: Raman spectra peaks: Plm/MWCNTs composite (blue) and MWCNTs (red)

### 3.2 Raman spectroscopy analysis results

The comparative Raman spectra of Plm/MWCNTs nanocomposite and MWCNTs are shown in Figure 2. Low frequency peaks (less than  $200\text{ cm}^{-1}$ ) observed in MWCNTs ( $966\text{ cm}^{-1}$ ) and  $977\text{ cm}^{-1}$  for Plm/MWCNTs are assigned to the  $A_{1g}$  symmetry radial breathing mode (RBM). The frequency of this mode rely solely on the tube diameter while the complete description of tube chiral indices can be deduced from resonant Raman measurements by using information tabulated in the Kataura plot for allowed excitations [21].

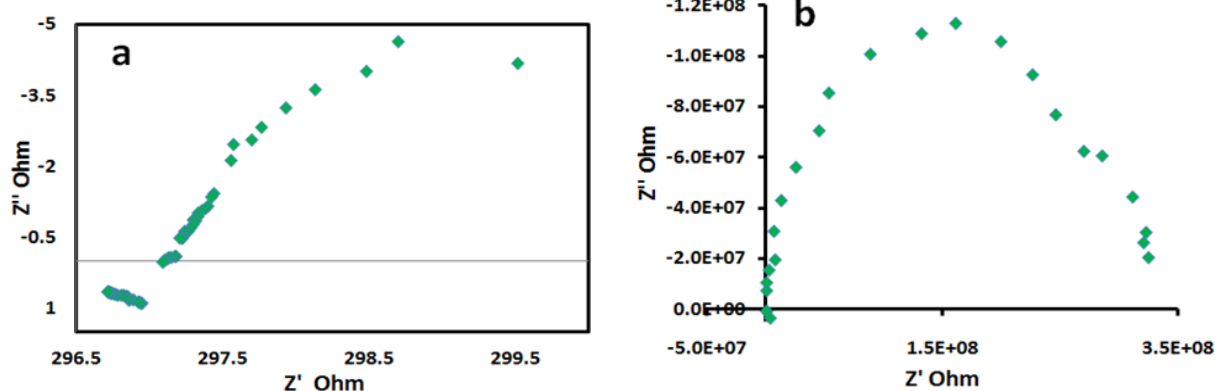


Fig. 3: Nyquist plots for bare carbon nanotubes (a) and Plm/MWCNTs composite (b)

The Raman spectrum of Plm/MWCNTs shows the so-called D-band and G-band peaks at  $1355\text{ cm}^{-1}$  and  $1593\text{ cm}^{-1}$ , respectively. The G-band peak is attributed to the C–C vibration with the  $sp^2$  hybridised orbital in graphene structures, whereas the D-band peak is attributed to disordered  $sp^2$  and non- $sp^2$  carbon defects in graphitic sheets. The D-band peak intensity, compared with that of the G-band peak, is a measure of the crystallinity of MWCNTs [22-23].

Earlier studies have revealed that SWCNTs displayed a radial breathing mode (RBM) with a wavenumber at  $100\text{--}200\text{ cm}^{-1}$ . The nonexistence of RBM mode in the Raman spectrum indicates that the presence of SWCNTs can be ruled out, and therefore, the product of the synthesised material is dominated by MWCNTs [24-25].

The two main typical graphite bands are present in the Raman spectrum of MWCNTs bundles: the band at  $1337\text{ cm}^{-1}$  (G band) assigned to the in-plane vibration of the C–C bond (G band) with another peak at  $1603\text{ cm}^{-1}$ , typical of defective graphite-like materials and the band at  $1355\text{ cm}^{-1}$  (D band) activated by the presence of disorder in carbon systems. The Raman spectrum also exhibits a band at  $2715\text{ cm}^{-1}$  called the  $G''$  band and attributed to the overtone of the D band. One of the striking features of the Raman spectra of  $sp^2$  carbon materials is the linear laser excitation energy dependence of the wavenumber of the

D and  $G''$  bands. Their strong dispersive behaviour has been largely interpreted as a double resonance process involving a laser-induced resonant transition of an electron from the valence to the conduction band of carbon materials [26-27]. A scattered resonance can take place if the electron is scattered by a phonon to a real state and after an elastic scattering process by lattice defects, the electron relaxes to the valence band [28]. Similar to FTIR the Raman spectroscopy results have also proved the formation of the hybrid Plm/MWCNTs composite.

### 3.3 Electrochemical impedance spectroscopy (EIS) characterisation

EIS measurements were carried out for further characterization of the Plm/MWCNTs composite. Figure 3 shows the Nyquist plots for the CNTs bare and the modified Plm/

MWCNTs composite. The Nyquist plot consists of a semi-circular part at high frequencies, whose diameter represents the charge transfer resistance  $R_{ct}$ , and a linear part at low frequencies, indicative of systems with diffusion-controlled current [29]. The semicircle diameter, which depends on the insulating features and dielectric at the electrode-electrolyte interface, can reveal its properties. The EIS data were fitted and the corresponding equivalent circuits are reported in Figure 3.

In this work Electrochemical impedance measurements were conducted by applying 10 mV on the sample of bare CNTs with a frequency range of between 4 Hz to 10 KHz, and measuring the alternative current. According to the Nyquist plot for bare carbon nanotubes (Figure 3a), it has been demonstrated that the real part was bigger than the imaginary part. The real resistance for CNTs was 297 Ohm.

Figure 3b, displays the EIS of Plm/CNTs hybrid material with two resistances real and imaginary parts. Any voltage applied inside the sample will lead to two current flows, the first one refers to assemblage of charges at Pt/Plm/CNTs and the second one, points to the charges out of electrode (Pt-contact) and through the CNTs hybrid film. It's worth knowing that both Pt/Plm/CNTs and Plm/CNTs signified the capacitors in the electrical circuit. From figure 3b the largest semicircle was obtained with Plm/CNTs (probably because of the interconnected nanoporous structure, suitable for facile electron transport) film which corresponds to a film resistance on the real axis of 350 M $\Omega$  which is an indication of a higher electron transfer rate in the redox probe and good electrical behaviour [30].

### 3.4 Cyclic Voltammetry (CV) characterisation

The Plm/MWCNTs hybrid composite solution was electrochemically characterised

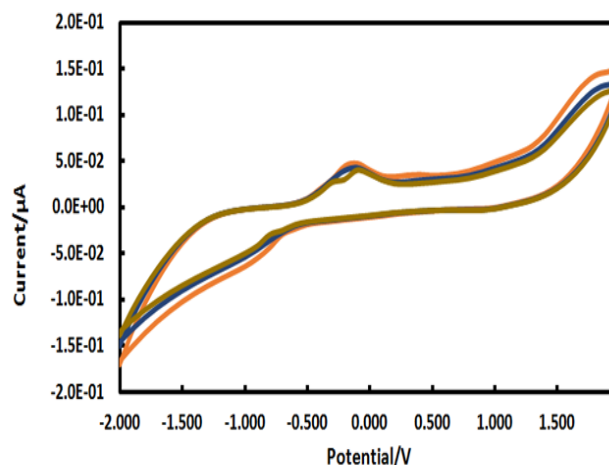


**Fig. 4: Cyclic voltammograms of the Plm/CNTs composite film at same scan rate on microband electrodes.**

by using cyclic voltammetry experiments (displayed in figure 4) with scan rate 0.05 v/s, voltage window (-0.5 – 0.7) Volt and current range between 1 to 100  $\mu$ A and the sample was deposited on microband electron. It shows a reversible wave that is the typical behaviour of conductive surfaces in the presence of the redox couple.

All CVs show a couple of redox peaks with a large increase of the anodic and cathodic peak currents and a decrease of the peak-to-peak separation, after electrode modifications, due to the increase of the electroactive surface area and reversibility of the systems, in both cases [30] found a significant enhancement in the redox peak currents for the plasma treated MWCNTs composites of hydrogen and ammonia, that is, they were having increments by 1.35 and 1.5 folds for anodic peak current, while the cathodic peak current shows the increments of 1.65 and 1.66 folds, respectively. They attributed the improvement of the current signals to the increment of the diffusion rate of MWCNTs composite and larger effective surface area that improved the sensitivity of the nanotubes' surfaces as compared to the bare MWCNTs [31]. In another work, it was discovered that CNTs/MnO<sub>2</sub> composite materials exhibited higher capacitive current than CNTs sheet in both H<sub>2</sub>SO<sub>4</sub> and Na<sub>2</sub>SO<sub>4</sub>

electrolytes, indicating that the total capacitance is as a result of MnO<sub>2</sub> pseudo-capacitance and EDLC capacitance [32-33]. The cyclic voltammetric results have revealed Plm/CNTs composite to have electrical conductance and can be used for sensing.

#### 4. Conclusion

Conductive polymer (Polyimidazole) multi-walled carbon nanotubes (MWCNTs) nanocomposite film were synthesised by chemical oxidation of imidazole monomer and addition of MWCNTs to the conductive polymer (CP) solution in 1:1 ratio. Chemical characterisation using FTIR revealed there is an increased in intensity of peaks in the control sample from 2823 and 2937 cm<sup>-1</sup> to 2833 and 2947 cm<sup>-1</sup> in Plm/MWCNTs composite respectively and Raman spectroscopy in which Plm/MWCNTs shows the so-called D-band peaks at 1355 cm<sup>-1</sup> and 1593 cm<sup>-1</sup>, both chemical analysis above confirmed the mixing of the polymer and the MWCNTs. Electrical measurements with current voltammetry (CV) that shows a reversible wave that is the typical behaviour of conductive surfaces in the presence of the redox couple and Impedance measurements in which the largest semicircle was obtained with Plm/CNTs film that corresponds to a film resistance on the real axis of 350 MΩ which is an indication of a higher electron transfer rate in the redox probe and good electrical behaviour. The overall results have shown that the composite has a significant electrical conductivity and can be applied in sensing volatile organic compounds in the environment.

#### References

- [1] Ryabchikova, E. (2021). Advances in Nanomaterials in Biomedicine. *Nanomaterials*, 11(1), 118. doi: 10.3390/nano11010118
- [2] Korotcenkov, G. (2020). Current Trends in Nanomaterials for Metal Oxide-Based Conductometric Gas Sensors: Advantages and Limitations. Part 1: 1D and 2D Nanostructures. *Nanomaterials*, 10(7), 1392. doi: 10.3390/nano10071392
- [3] Abdul Samad, M. (2021). Recent Advances in UHMWPE/UHMWPE Nanocomposite/UHMWPE Hybrid Nanocomposite Polymer Coatings for Tribological Applications: A Comprehensive Review. *Polymers*, 13(4), 608. doi: 10.3390/polym13040608
- [4] Thompson, H. (2017). *Polymer Nanocomposites*. Hauppauge: Nova Science Publishers, Inc.
- [5] Banisaeid, M. (2020). Effect of functionalized carbon nanotubes on the mechanical properties of epoxy-based composites. *Fullerenes, Nanotubes And Carbon Nanostructures*, 28(7), 582-588. doi: 10.1080/1536383x.2020.1724966
- [6] Zhang, H., Zhou, Z., Qiu, J., Chen, P., and Sun, W. (2021). Defect engineering of carbon nanotubes and its effect on mechanical properties of carbon nanotubes/polymer nanocomposites: A molecular dynamics study. *Composites Communications*, 28, 100911. doi: 10.1016/j.coco.2021.100911
- [7] Banisaeid, M. (2020). Effect of functionalized carbon nanotubes on the mechanical properties of epoxy-based composites. *Fullerenes, Nanotubes And Carbon Nanostructures*, 28(7), 582-588. doi: 10.1080/1536383x.2020.1724966
- [8] Kuang, D., Hou, L., Wang, S., Luo, H., Deng, L., and Mead, J. et al. (2019). Large-scale synthesis and outstanding microwave absorption properties of carbon nanotubes coated by extremely small FeCo-C core-shell nanoparticles. *Carbon*, 153, 52-61. doi: 10.1016/j.carbon.2019.06.105
- [9] Athawale, P., Kashinath, K., and Reddy, D. (2016). Enantiospecific Formal Synthesis of Inthomycin C. *Chemistryselect*, 1(3), 495-497. doi: 10.1002/slct.201600128
- [10] Kulkarni, S., Patil, P., Mujumdar, A., and Naik, J. (2018). Synthesis and evaluation of gas sensing properties of PANI, PANI/SnO<sub>2</sub> and PANI/SnO<sub>2</sub>/rGO nanocomposites at room temperature. *Inorganic Chemistry Communications*, 96, 90-96. doi: 10.1016/j.inoche.2018.08.008
- [11] Sreenath, P., Mandal, S., Singh, S., Panigrahi, H., Das, P., Bhowmick, A., and Dinesh Kumar, K. (2020). Unique approach to debundle carbon nanotubes in polymer matrix using carbon dots for enhanced properties. *European Polymer Journal*, 123, 109454. doi: 10.1016/j.eurpolymj.2019.109454
- [12] Kausar, A. (2016). Carbon nano onion as a versatile contender in polymer compositing and advanced application. *Fullerenes, Nanotubes And Carbon Nanostructures*, 25(2), 109-123. doi: 10.1080/1536383x.2016.1265513
- [13] Gerasimov, G. (2021). Dispersion, Photochemical Conversion and Bioaccumulation of Pollutants near Highway. *Physical-Chemical Kinetics In Gas Dynamics*, 22(4), 23-47. doi: 10.33257/phchgd.22.4.943
- [14] Lee, C., Tran, M., Choo, C., Tan, C., and Chiew, Y. (2020). Evaluation of air quality in Sunway City, Selangor, Malaysia from a mobile monitoring campaign using air pollution micro-sensors. *Environmental Pollution*, 265, 115058. doi: 10.1016/j.envpol.2020.115058
- [15] Kolosnjaj-Tabi, J., and Moussa, F. (2017). Anthropogenic Carbon Nanotubes and Air Pollution. *Emission Control Science And Technology*, 3(3), 230-232. doi: 10.1007/s40825-017-0065-3
- [16] Miramirkhani, F., and Navarchian, A. (2017). Morphology, Structure, and Gas Sensing Performance

- of Conductive Polymers and Polymer/Carbon Black Composites Used for Volatile Compounds Detection. *IEEE Sensors Journal*, 17(10), 2992-3000. doi: 10.1109/jsen.2017.2685180
- [17] Zheng, X., Ma, Z., and Zhang, D. (2020). Synthesis of Imidazole-Based Medicinal Molecules Utilising the van Leusen Imidazole Synthesis. *Pharmaceuticals*, 13(3), 37. <https://doi.org/10.3390/ph13030037>
- [18] Li, C., Yan, Z., Zhang, Y., Qi, L., Ge, S., and Shao, Q. (2020). Conductive waterborne silicone acrylate emulsion/carbon nanotubes composite coatings: preparation and characterization. *Fullerenes, Nanotubes And Carbon Nanostructures*, 29(7), 547-555. <https://doi.org/10.1080/1536383x.2020.1860947>
- [19] Korotcenkov, G. (2011). *Chemical Sensors Fundamentals of Sensing Materials* (1st ed., pp. 31-67). New York: Momentum Press.
- [20] Schneider, M., and Hase, F. (2009). Ground-based FTIR water vapour profile analyses. *Atmospheric Measurement Techniques*, 2(2), 609-619. doi: 10.5194/amt-2-609-2009.
- [21] S, N., IJ, A., and EC, A. (2017). Synthesis, FTIR and Electronic Spectra Studies of Metal (II) Complexes of Pyrazine-2-Carboxylic Acid Derivative. *Medicinal Chemistry*, 7(11). doi: 10.4172/2161-0444.1000475
- [22] Lehman, J., Terrones, M., Mansfield, E., Hurst, K., and Meunier, V. (2011). Evaluating the characteristics of multiwall carbon nanotubes. *Carbon*, 49(8), 2581-2602. doi: 10.1016/j.carbon.2011.03.028
- [23] Verma, S., Choudhury, A., and Kar, P. (2017). Selective Sensing of Ethanol by Poly(m-aminophenol)/Amine Groups Functionalized Multi-Walled Carbon Nanotube Composite. *Sensor Letters*, 15(5), 448-456. doi: 10.1166/sl.2017.3826
- [24] Hung, N., Chinh, N., Nguyen, T., Kim, E., Choi, G., Kim, C., and Kim, D. (2020). Carbon nanotube-metal oxide nanocomposite gas sensing mechanism assessed via NO<sub>2</sub> adsorption on n-WO<sub>3</sub>/p-MWCNT nanocomposites. *Ceramics International*, 46(18), 29233-29243. doi: 10.1016/j.ceramint.2020.08.097
- [25] Kobayashi, K., Kitaura, R., Kumai, Y., Goto, Y., Inagaki, S., and Shinohara, H. (2008). Synthesis of single-wall carbon nanotubes grown from size-controlled Rh/Pd nanoparticles by catalyst-supported chemical vapour deposition. *Chemical Physics Letters*, 458(4-6), 346-350. doi: 10.1016/j.cplett.2008.05.016
- [26] Hou, P., Song, M., Li, J., Liu, C., Li, S., and Cheng, H. (2015). Synthesis of high quality nitrogen-doped single-wall carbon nanotubes. *Science China Materials*, 58(8), 603-610. doi: 10.1007/s40843-015-0074-x
- [27] Kürti, J., Zólyomi, V., Grüneis, A., and Kuzmany, H. (2002). Double resonant Raman phenomena enhanced by van Hove singularities in single-wall carbon nanotubes. *Physical Review B*, 65(16). doi: 10.1103/physrevb.65.165433
- [28] Brown, S., Jorio, A., Dresselhaus, M., and Dresselhaus, G. (2001). Observations of the D-band feature in the Raman spectra of carbon nanotubes. *Physical Review B*, 64(7). doi: 10.1103/physrevb.64.073403
- [29] Reich, S., and Thomsen, C. (2004). Raman spectroscopy of graphite. *Philosophical Transactions Of The Royal Society Of London. Series A: Mathematical, Physical And Engineering Sciences*, 362(1824), 2271-2288. doi: 10.1098/rsta.2004.1454
- [30] Wang, T., Reid, R., and Minter, S. (2015). A Paper-based Mitochondrial Electrochemical Biosensor for Pesticide Detection. *Electroanalysis*, 28(4), 854-859. doi: 10.1002/elan.201500487
- [31] Tortellini, C., Tasca, F., Venneri, M., Marchese, C., and Antiochia, R. (2021). Gold Nanoparticles/Carbon Nanotubes and Gold Nanoporous as Novel Electrochemical Platforms for L-Ascorbic Acid Detection: Comparative Performance and Application. *Chemosensors*, 9(8), 229. doi: 10.3390/chemosensors9080229
- [32] Abdul Rahim, Z., Yusof, N., Mohammad Haniff, M., Mohammad, F., Syono, M., and Daud, N. (2018). Electrochemical Measurements of Multi-walled Carbon Nanotubes under Different Plasma Treatments. *Materials*, 11(10), 1902. doi: 10.3390/ma11101902
- [33] Dawoud, H., Al Tahtamouni, T., and Bensalah, N. (2019). Sputtered manganese oxide thin film on carbon nanotubes sheet as a flexible and binder-free electrode for supercapacitors. *International Journal Of Energy Research*, 43(3), 1245-1254. doi: 10.1002/er.4364